inter.noise 2014
MELBOURNE AUSTRALIA
16-19 NOVEMBER

Distance perception of a nearby virtual sound source reproduced by a linear loudspeaker array

Dong-Soo KANG[1]; Jung-Woo CHOI[2]; Yang-Hann KIM[3]; William L. MARTENS[4]

[1,2,3] Korea Advanced Institute of Science and Technology, Republic of Korea

[4] University of Sydney, Australia

ABSTRACT

When a virtual sound source is reproduced by a linear loudspeaker array, listeners can perceive not only the direction of the source, but also its distance. Control over perceived distance has often been implemented via the adjustment of various acoustic parameters, such as loudness, spectrum change, and the direct-to-reverberant energy ratio; however, there is a neglected yet powerful cue to the distance of a nearby virtual sound source that can be manipulated for sources that are positioned away from the listener's median plane. By extending the manipulation of interaural level difference (ILD) to lower frequencies than what is typical for such lateralized sources, a very strong means becomes available for controlling perceived distance of sources at close range, within the listener's peripersonal space (within arm's reach). Of course, the ILD of a virtual source reproduced by a line array will not be identical to that of a real monopole, due to many physical limitations such as finite aperture, spatial aliasing and stationary phase approximation. Using an ideal rigid sphere as a model of the variation in head-related transfer functions at close range, this paper identifies the effects of these artifacts on perception of the nearby virtual source.

Keywords: sound field reproduction, virtual source, line array, distance perception, interaural level difference
I-INCE Classification of Subjects Number(s): 74.9

1. INTRODUCTION

Virtual Sound Source Reproduction, which means the reproduction of a desired sound source (which does not actually exist) over a finite area by a loudspeaker array, can deliver spatial sound impressions to multiple listeners (1). There are two types of virtual sources, one is a virtual-source-outside, which is located outside an enclosed array, and the other is a virtual-source-inside (2) (or a focused source (3, 4)), which is located inside an array, that is, on the same side of the array as the listener's position. What we deal with in this paper is the virtual-source-inside type, because it is an improvement method which is proposed that allows a source to be reproduced in the listener's peripersonal space (within arm's reach).

While the Kirchhoff-Helmholtz integral (K-H integral) can provide a theoretical foundation for the virtual-source-outside case, a general solution to generate virtual-source-inside is regarded as impossible due to physical limitations (1, 2). Reproduction in the virtual-source-inside case is hard to implement, but has many applications, such as a holographic display (5, Fig.1-3). For this reason, various methods have been advanced to reproduce a virtual-source-inside to overcome such limitations. In the approach taken in Wave Field Synthesis (6), a time reversal operator is used to synthesize the virtual-source-inside result (3). But a wave converging to the virtual source position is also reproduced as an artifact (1). Therefore a truncation method is applied to reduce this artifact in the selected region. In the mode-matching approach (e.g., 7), the sound field in a region of interest is filtered in a wavenumber domain. Mode matching of this field is done by expansion of the coefficient. Choi and Kim (1) proposed a new approach to generate a virtual-source-inside result using an integral formula that can directly separate the region of interest from the artifacts. The virtual source is

[1] dooly0819@kaist.ac.kr
[2] khepera@kaist.ac.kr
[3] yanghann@kaist.ac.kr
[4] william.martens@sydney.edu.au

replaced by a compact multipole source that has directivity, and the driving signals of the control sources are derived using a time-reversal operator. (For the detailed explanations of these approaches, see (8).)

When a virtual source is located near the listener, what the listener perceives is not only the direction of the source, but also the distance. While the direction perception of a virtual source reproduced by a line array has been discussed in many studies, distance perception has been discussed in only a few (e.g., 9, 10). In this paper, we will discuss the distance perception characteristics of virtual sources that are located quite near to the listener.

In the case of reproducing a virtual source using a linearly distributed loudspeaker array (when the virtual-source-inside is located in front of an array, near the listener's region, as in Figure 1.), stationary phase approximation (SPA) is applied to approximate surface integral to line integral, which means linear distributed control sources can be used instead of enclosed arrays. By this reduction of the control source surface, several artifacts arise when reproducing the virtual source. These artifacts will also be discussed in this paper.

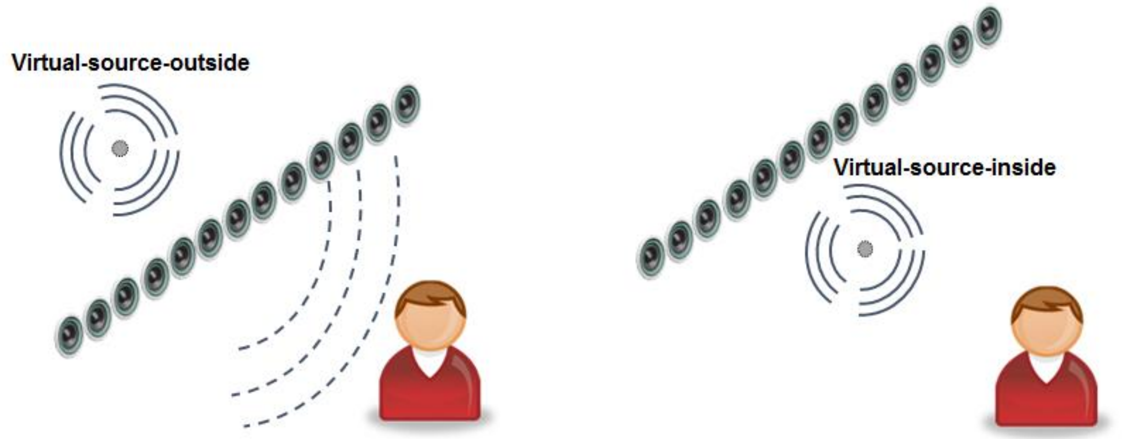

Figure 1 – a virtual-source-outside (left) and a virtual-source-inside (right) reproduced by a line array

2. PROBLEM DEFINITION

To discuss the perception of the distance of a virtual source reproduced by a line array, previous studies of distance perception are reviewed first. To compare a real sound source and the virtual source, the driving function of a virtual-source-inside case is briefly reviewed. Then the artifacts which are induced during the realization of a virtual-source-inside image are discussed and organized. Then the cues of distance perception are applied to analyze the resulting artifacts.

2.1 Distance Perception of a Sound

Prior to analyzing the perceptual characteristics of the virtual source, distance perception of a real sound source has to be studied. For a single sound source in space, listeners can perceive not only its frequency spectrum and intensity, but also its direction and distance. While there are many auditory cues to perceive distance, Coleman (11) suggests the most significant cues are loudness, reverberation and frequency spectrum, and also discusses the potential involvement of interaural differences. While loudness and frequency spectrum may often be confused with the sound pressure level and the spectrum of the sound source itself, these cues can be used if the listener has prior knowledge of the sound source or can relatively compare the sound with a reference (e.g., 12). The importance of reverberation as a cue to distance is also unquestionable. As shown in previous studies, the perception of the distance is hard without the presence of room reflection (13). In reverberant environments, direct to reverberant ratio can be a strong cue to perceive distance (e.g., 14). For distances at least over 1m, it is hard to judge the distance without loudness and reverberation cues (15).

When the source is located in the listener's near field (which is within 1m), interaural level difference (ILD) serves as an additional auditory cue to perceive distance for source sources that arrive at azimuth angles offset away from the listener's median plane (13). While interaural time difference (ITD) is not much changed with respect to the distance, ILD varies dramatically when the source is close to the listener's ear position, as much as 20dB for distances between 17.5cm and 87.5cm (16). Brungart and Rabinowitz (17, 18) found that low frequency (below 3 kHz) ILD is a strong auditory cue enabling judgements of source distance in an anechoic environment. Although Shinn-Cunningham et al. (19) found that adding reflection improves the distance perception significantly, ILD potentially could be the strongest cue to distance of a nearby virtual source when the sound field reproduction basically aims to reproduce direct sound from a virtual source.

The ILD can simply be defined by the ratio of sound pressure level of the listener's right and left ears. Without considering the scattering of the head, ILD induced by a point source located at distance r_v from the center of the head can be expressed as

$$ILD(r_v,\gamma,\omega) = 20\log_{10}\left|\frac{e^{jkr_R}}{r_R}\right| \Big/ \left|\frac{e^{jkr_L}}{r_L}\right| = 20\log_{10}\left(\frac{r_L}{r_R}\right) \tag{1}$$

where r_R and r_L are the distances from the source to right and left ear, k is a wavenumber, and γ is the angle between the left ear and the source. ILD by a point source simply depends on the ratio of propagation paths to listener's two ears. Figure 2 shows the geometry and ILD with respect to the distance and relative angle from a point source.

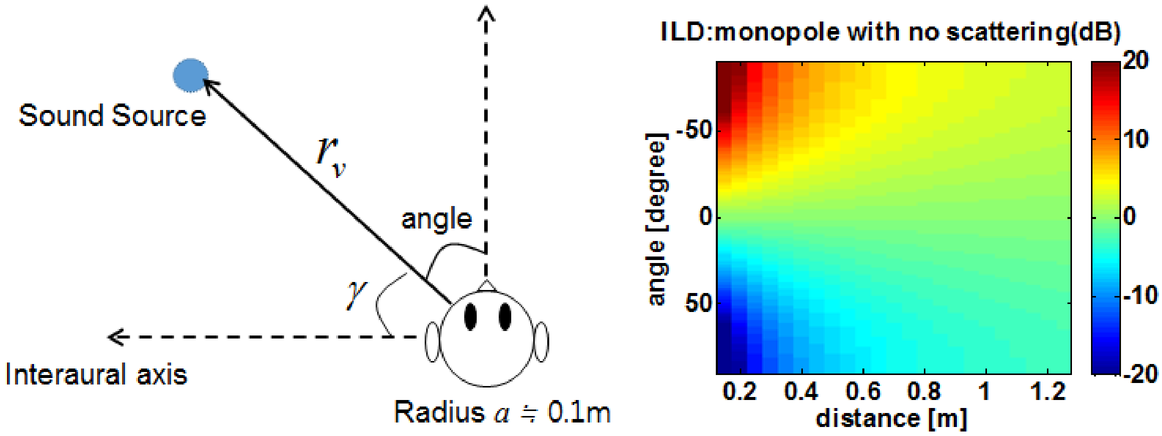

Figure 2 – (left) geometry used in ILD formulation (right) no-head ILD over distance and the angle

We find that when the source is positioned away from the listener's median plane, ILD increases with respect to the distance of the source. ILD is always zero when the source is in front of the listener, since the lengths of the propagation paths to two ears are always same.

But this model doesn't consider the presence of the head, which interferes with the propagation of the wave. When considering human's head scattering, ILD characteristics become complex with respect to its frequency. Using the rigid sphere model (20) which is validated with the bowling ball head (21), Brungart and Rabinowitz (22) found that the rigid sphere model can approximately considered as a human's head-related transfer function (HRTF) at the frequency below 1kHz. For the higher frequencies, real HRTF is affected by obstacles such as pinna (23). The expression for the scattered sound pressure at the ear excited by a point source used in this paper is given by

$$P(r_v,\gamma,\omega) = -\frac{1}{4\pi ka^2}\sum_{n=0}^{\infty}(2n+1)\frac{h_n^{(1)}(kr_v)}{h_n'^{(1)}(ka)}P_n(\cos\gamma), \tag{2}$$

where a is the radius of a head, P_n is the Legendre polynomial function and h_n is the spherical Hankel function. Assuming that ears are located at diametrically opposed points on the surface of the head, ILD can be expressed as

$$ILD(r_v,\gamma,\omega) = 20\log_{10}\left|\sum_{n=0}^{\infty}(-1)^n(2n+1)\frac{h_n^{(1)}(kr_v)}{h_n'^{(1)}(ka)}P_n(\cos\gamma)\right| \Big/ \left|\sum_{n=0}^{\infty}(2n+1)\frac{h_n^{(1)}(kr_v)}{h_n'^{(1)}(ka)}P_n(\cos\gamma)\right| \tag{3}$$

Considering head-scattering, ILDs at several frequencies are shown as Figure 3. This figure reveals that ILD increases as the source angle approaches that of the ear, and decreases as it rotates away from the ear. ILD also increases with frequency when there are direct paths between the source and two ears, and decreases at one point due to an interesting phenomenon in the acoustic shadow of the spherical head. This phenomenon is called the acoustic bright spot, which arises when an ear is located directly opposite the source, which means that γ is 180°. All sound propagation paths from the source to the ear are spherically symmetric, and all diffracted sound waves combine in phase at the position of the ear. As the frequency increases, these effects are seen as ripples. Brungart and Rabinowitz (22) found that this sphere model fits the KEMAR measurements at the frequencies below 1 kHz. Above this frequency, KEMAR results begin to diverge from the sphere model.

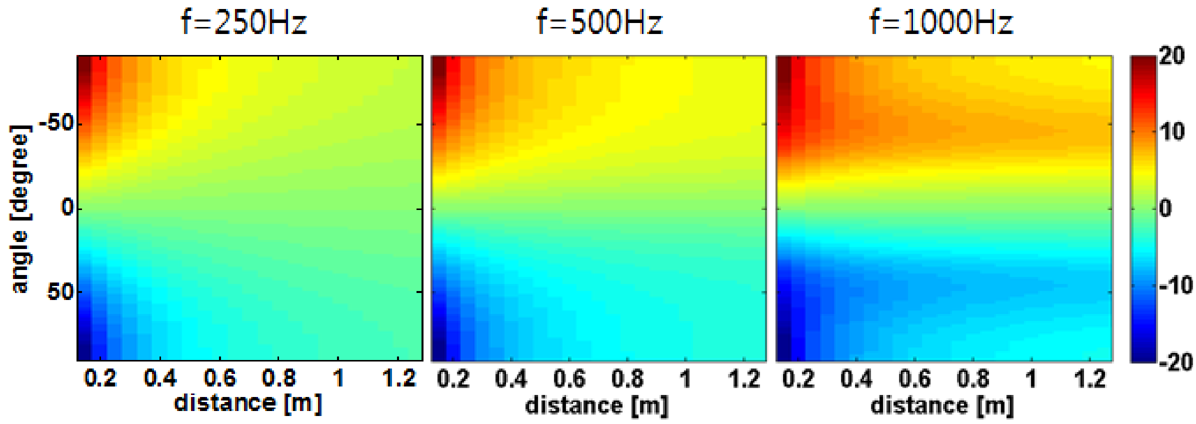

Figure 3 – ILD considering rigid sphere model (dB scale). (left) 250Hz (center) 500Hz (right) 1 kHz

From these previous studies, we can conclude that ILD could be a dominant cue for the perception of distance within 1m, and that below 1 kHz, we can use rigid sphere model to simulate the human’s head scattering.

2.2 Reproduction of a Virtual-source-inside by a Line Array

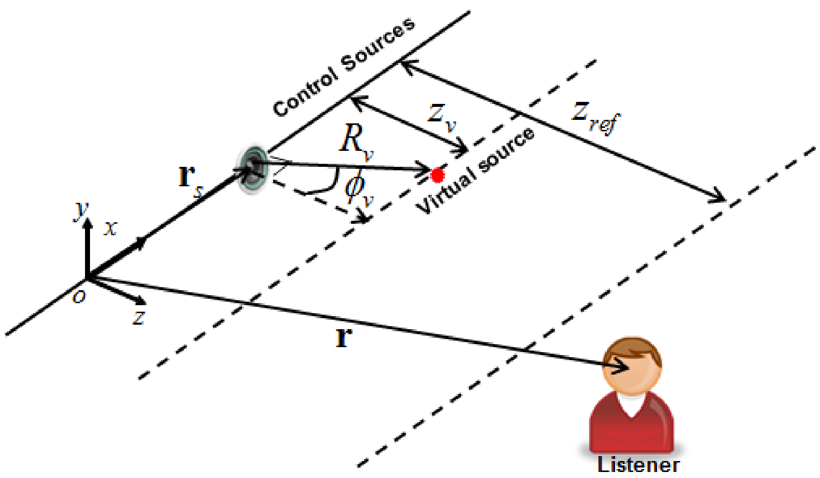

Figure 4 – Illustration of the geometry and variables used in the formulation ($\mathbf{r}_s$: control source position, $\mathbf{r}$: listener’s position, R_v: distance between a control source and a virtual source, z_v: z-direction component of R_v, : distance of reference line, : angle between R_v and z_v)

Unlike the conventional theories that can reproduce a virtual-source-outside, virtual-source-inside needs a different approach. Boone et al. (3, 4) showed that an approximated K-H integral can reproduce the wavefront from a virtual source in front of a line array with time-reversal techniques (4). However, there’s a problem where the wavefront that is converging to the location of the virtual source always exists as an artifact when the control sources surround the listener. But this artifact is less problematic when the line array is used, because the region in which the wave converges to the virtual-source-inside is separated from the region of interest (where the listeners are located.)

2.2.1 Applying stationary phase approximation

Initial formulation of the virtual-source-inside is derived from Rayleigh's first integral with time-reversed source (4), considering infinite planar distribution of monopole control sources. When the virtual source and the listener is located at the same plane, a line array can be used instead of the planar array by applying SPA (e.g., 24). Reproduced pressure field can be written as

$$P(\mathbf{r},\omega) = \int_{-\infty}^{\infty} \frac{z_v}{R_v} \sqrt{\frac{ik}{2\pi} \frac{z_{ref}}{z_{ref} - z_v}} \frac{e^{-ikR_v}}{\sqrt{R_v}} G(\mathbf{r}|\mathbf{r}_s,\omega)\, dl(\mathbf{r}_s). \tag{4}$$

Variables can be found in Figure 4, except $G(\mathbf{r}|\mathbf{r}_s,\omega)$, which is a free-field Green's function serving as a transfer function from the control source to the listener's position. When replacing free-field Green's function with the scattered pressure described in equation (2) for each of control sources, the head scattered pressure field reproduced by a line array can be calculated. Note that z_{ref} is a distance between control sources and a reference line, with the listener supposed to be in that line. Due to the stationary phase approximation, reproduction results only hold in this line. Detail derivation process can be found in (4).

The first problem that causes an artifact comes from SPA. A condition to apply SPA is that the phase term of the integral has to be changed rapidly along the integration section, which is equivalent to

$$k(|\mathbf{r}-\mathbf{r}_s| - Rv) >> 1, \tag{5}$$

meaning that the distance between the listener and the virtual source has to be large compared to the wavelength. This condition is hard to be satisfied at lower frequencies. It can be concluded that if the virtual source reproduced by a line array is located nearby a listener, the reproduced field may not be equivalent to that of the real point source located at the position of the virtual source. To satisfy the condition of SPA (equation (5)) at the low frequencies, the distance between the virtual source position and the listener has to be as large as possible. When the source is close to the head (which is the objective of nearby virtual source), this condition will break down.

To simulate the effect of SPA, normalized squared error is defined to identify the magnitude of the reproduction error (2) as

$$\varepsilon(\mathbf{r}) = \left| p_{monopole}(\mathbf{r}) - p_{virtualsource}(\mathbf{r}) \right|^2 \Big/ \left| p_{monopole}(\mathbf{r}) \right|^2, \tag{6}$$

where $p_{virtualsource}$ denotes the reproduced field by a line array and $p_{monopole}$ is ideal monopole's sound field. Errors are shown in dB scale. Black area represents the region where the relative error is less than -20dB, which is equivalent to 1% error and can be seen as a region of good reproduction quality (25).

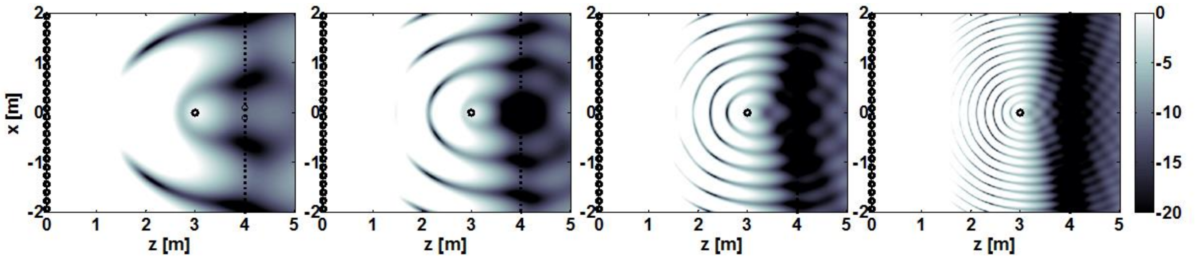

Figure 5 – Normalized squared error plot of a virtual source reproduced by a line array positioned 1m from the listener's line (frequency: 125Hz, 250Hz, 500Hz, 1kHz (from the left))

Figure 5 shows the normalized error plot when the listener and reference line are located 4m from an array with length of 244m, which can be assumed and checked as an infinite aperture. The number of control sources is 1440, which the gap between control sources can prevent spatial aliasing artifact below 1 kHz. Reproduced frequencies are 125Hz, 250Hz, 500Hz and 1 kHz, from the left figure. At the reference line ($z = z_{ref}$=4m), No errors occur since the condition of SPA is satisfied. When the frequency decreases, which means that the wavenumber also decreases, error at the reference line becomes larger. Figure 6 shows the relative errors for different distances of a virtual source with the frequency of 500Hz. The location of the black dot represents the location of a virtual source, which is 0.25m, 0.5m, 1m and 2m from the listener's line respectively. When the virtual source is close to the listener, magnitude error arises.

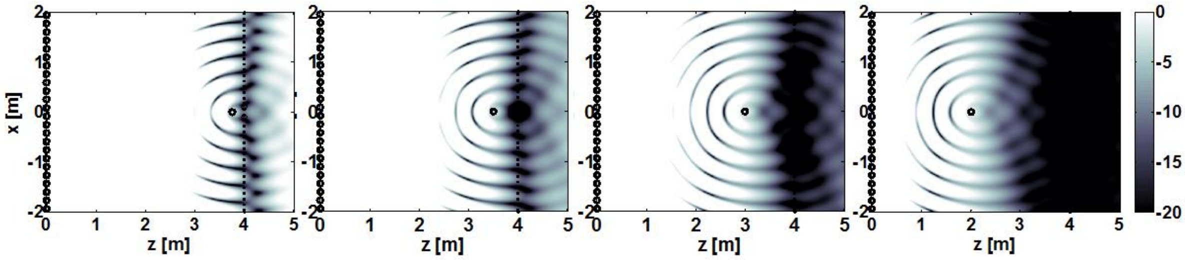

Figure 6 – Normalized squared error plot of a virtual source reproduced by a line array

(frequency: 500Hz, distance from the listener's line: 0.25m 0.5m, 1m, 2m (from the left))

2.2.2 Effect of finite aperture

The second problem comes from the physical limitation that infinite length of a line array is practically impossible. Due to the limitation of space and number of control sources, we can only use finite number of control sources with finite aperture. Reconstruction area is set by this limitation. When there's no control source on the extended line that connects the virtual source and the listener's position (which is equivalent to a stationary phase point), the listener cannot get a spatial impression of the virtual source. Figure 7 shows the reconstruction area. Considering two ear positions, possible positions of virtual source can be seen on the right side of the figure. As seen in the figure, virtual source cannot be positioned when the source is really close to the listener.

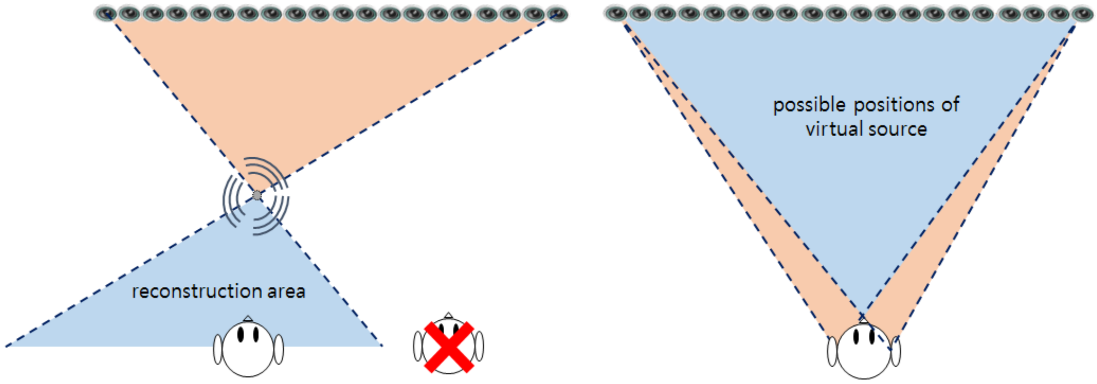

Figure 7 – Conceptual illustrations of artifacts due to a finite aperture (left) reconstruction area (blue) for a certain position of virtual source (right) possible positions of virtual source for a certain listener

The equation for a sound field reproduced by a line array with the length of L can be written as

$$P(\mathbf{r},\omega) = \int_{-L/2}^{L/2} \frac{z_v}{R_v} \sqrt{\frac{ik}{2\pi} \frac{z_{ref}}{z_{ref} - z_v}} \frac{e^{-ikR_v}}{\sqrt{R_v}} G(\mathbf{r}|\mathbf{r}_s,\omega)\, dl(\mathbf{r}_s). \tag{7}$$

Diffraction artifacts are also caused by this finite aperture. When replacing infinite integral with finite integral, a rectangular window is applied to the resultant driving function of the control sources, which causes a comb-filtering effect. (Details can be found in (20), p. 319.) To reduce this artifact, spatial tapering is applied to the driving function of control sources, which reduces ripples in sound field with the expense of narrowing angle of reconstruction area. In this paper, 1/4th cosine tapering window is applied to reduce artifacts.

Figure 8 shows the normalized error plot, when the listener is located 1m from an array with various array apertures. Changing the number of control sources by 10 times results in changes in relative error, as can be seen as the figure. It can be shown that when the array length is about 3.9m, which is readily implemented, almost all positions have large errors when the source is close to the listener. These errors may be found to cause variation in perceived virtual source distance.

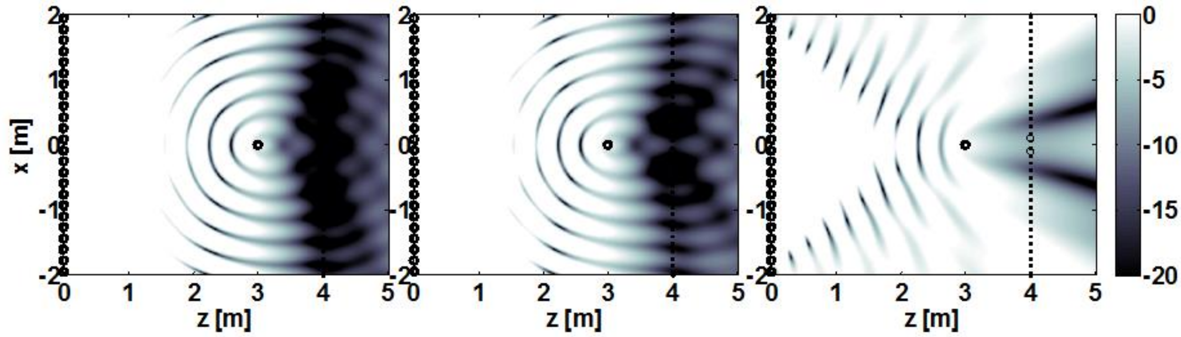

Figure 8 – Normalized squared error plot of a virtual source reproduced by a line array positioned 1m from the listener (frequency: 500Hz, array length: 406.8m (left), 40.5m (center), 3.9m (right) which is equivalent to the number of sources: 2400 (left), 240 (center), 24 (right))

2.2.3 Effect of discretization

Due to the limitation of the number of control sources, discretized arrays has to be used. A discrete distribution of control sources produces artifact while there's not by a continuous distribution, which is well-known spatial aliasing. Reproduced sound field with the uniformly discretized N control sources can be written as

$$P(\mathbf{r},\omega)=\sum_{n=1}^{N}\frac{z_v}{R_v^{(n)}}\sqrt{\frac{ik}{2\pi}\frac{z_{ref}}{z_{ref}-z_v}}\frac{e^{-ikR_v^{(n)}}}{\sqrt{R_v^{(n)}}}G(\mathbf{r}\big|\mathbf{r}_s^{(n)},\omega)\,\Delta\mathbf{r}_s, \tag{8}$$

where $\Delta\mathbf{r}_s$ is a gap between each control source and subscript (n) denotes the source numbering. This can also be expressed as multiplying impulse train with the gap of $\Delta\mathbf{r}_s$, then the sampling theorem can be applied. When $\Delta\mathbf{r}_s$ is smaller than half of the wavelength, this spatial aliasing artifact can be avoided due to the sampling theorem, which means that dense spatial sampling is required at higher frequencies. The effect of discretization on distance perception will be discussed in future work.

3. SOLUTION METHOD

Based on the previous studies, ILDs of a virtual source and a real source considering head-scattering, but no reverberation, are compared to distinguish the near-field distance perception characteristics of the virtual source reproduced by a line array.

3.1 Effect of Stationary Phase Approximation

Configuration of the array to be considered here is the same as for the array of 2.2.1, which allows us to ignore the artifacts of finite aperture and discretization. Figure 9 shows the ILD map considering the head scattering effect at the frequencies of 250Hz, 500Hz and 1 kHz. The listener is assumed to face the line array. Comparing with Figure 3, characteristics of ILD with respect to the distance and the angle of the virtual source is quite different. Figure 10 shows the ILD difference for monopole and virtual sources reproduced by the line array, simply subtracting the ILD of the monopole (Figure 3) from the ILD of the virtual source (Figure 9). It can be shown that when the virtual source is close to the listener, the ILD error increases. When the frequency decreases, ILD errors at the near field increases. When the angle between a virtual source and a listener becomes larger, error arises much in the region that the ILD cues become dominant to perceive distance, as can be seen in equation (5). It can be concluded that distance perception characteristics of a virtual source reproduced by a line array is not the same as the real monopole even though the length of an array is long enough.

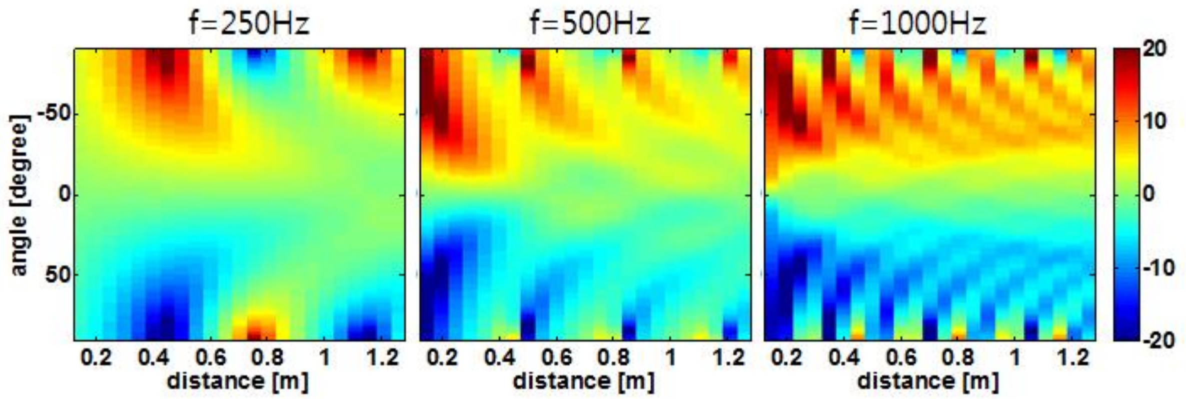

Figure 9 – ILD of virtual source. Frequency: (left) 250Hz (center) 500Hz (right) 1 kHz

When the absolute magnitude of virtual source's ILD is larger than a monopole, listener may perceive the distance to be closer, assuming ITD is well-reproduced. When absolute magnitude of a virtual source's ILD is smaller than that of a monopole, listener may perceive the distance to be larger. As can be seen in Figure 9, sign of ILD error is not equal when the artifact arises, we can hardly estimate the total perceptual character as described before. When we hear not a single frequency sound but spectrum (which make distance perception more precise), these ripples can be lumped together.

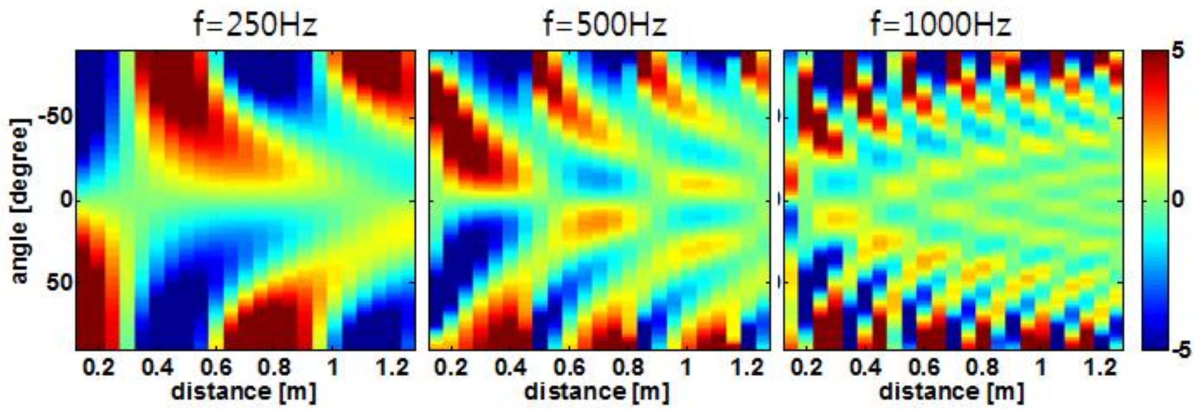

Figure 10 – (ILD of virtual source) – (ILD of monopole). Frequency: same as Figure 9.

When the frequency becomes larger, we can expect that the ILD of a virtual source becomes more similar to that of a monopole. While the rigid sphere model can only simulate human's head under 1 kHz, real HRTF has to be consider the frequency range of 1kHz to 3kHz (the highest frequency that ILD cue is dominant to perceive distance).

These results are based on the assumption that the listener is facing the center of the array, meaning that both ears are located at the same (reference) line. When the ears are not located at the same line, another artifact arises, even when the far-field condition of SPA is satisfied.

Applying one more SPA to the equation (4), we can reduce line integral to a certain value. The condition of equation (5) has to be satisfied also with this approximation. Then the resultant pressure field can be expressed as

$$P(\mathbf{r},\omega)=\sqrt{\frac{z_{ref}}{z_{ref}-z_v}}\sqrt{\frac{z-z_v}{z}}\frac{e^{ikR}}{R}. \tag{9}$$

R denotes the distance between the location of a virtual source and a listener's ear and z denotes the z-direction component of listener's ear position. When the listener is not seeing an array, z of both ear is different to each other. Comparing equation (9) with the monopole located at the same position ($P(\mathbf{r},\omega)=e^{ikR}/R$), each doubling of the distance does not meet the decrease of 6dB. These artifact was discussed by Wittek et al., but the condition of SPA doesn't meet with this equation.

3.2 Effect of Finite Aperture

Due to a finite aperture, diffraction artifacts come into the listener's area. Then the possible position of a virtual source is limited as can be seen in Figure 7.

Figure 11 shows the ILD with respect to the position of a virtual source, when reproduced by a line array with the length of 3.9m (24 control sources). Considering a listener located at 4m from the array, where angles of possible position of a virtual source are narrow compared with previously examined cases. When the source is located at the distance of 0.2m from a listener, there is no possible position of a virtual source. When the source is located at 1m (which is the maximum distance that uses ILD as a distance perception cue), the angle is about ±26°. When the virtual source is located out of this area, what we can hear is an artifact.

Note that the color axis of the right map of Figure 11 is larger than Figure 10. This means that the artifacts due to a finite aperture are larger than the artifacts due to the stationary phase approximation. In binaural hearing, the angle and the nearest position is limited when the aperture is finite.

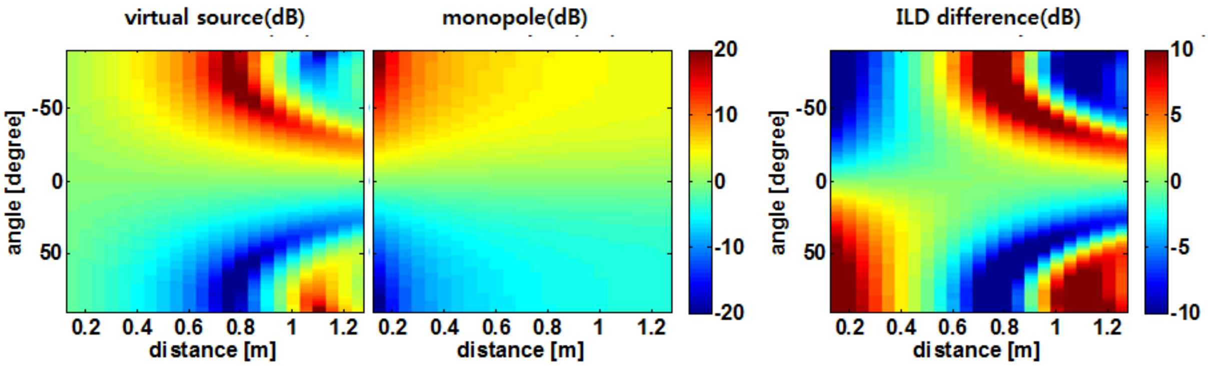

Figure 11 – (left) ILD of a virtual source reproduced by a short line array (center) ILD of a real monopole source (right) (ILD of virtual source) – (ILD of monopole). Frequency: 500Hz

4. CONCLUSIONS

To examine the potential for controlling the perceived distance of a virtual source reproduced by a line array, Interaural Level Difference (ILD) was chosen over other cues since others depend more on the characteristics of the signal itself or the reverberation. ILD under 3kHz can be a strong cue to the distance of nearby sources, particularly those within 1m. Using a rigid sphere model that simulates the human head transfer function under 1kHz, the ILD of the virtual source can be included in the reproduction by line array.

A key method that can reduce surface integral (which can fully reproduce the sound field of a virtual source) to a line integral relies upon far-field conditions at high frequencies, and these conditions do not meet the requirements for the control of distance perception for a nearby source. Also a practical limitation of the number of control sources leads to the reduction of the length of the line array and extention of the the gap between each control source. This can causes artifacts such as a diffraction artifact and an aliasing artifact. The diffraction artifact causes not only the lowering of the reproducible angle of a virtual source, but also limits control over distance. The aliasing artifact has to be considered also, and will be discussed in future works.

ACKNOWLEDGEMENTS

This work was supported by the Ministry of Trade, Industry and Energy (MOTIE) grant funded by the Korea government (No. 10037244), and the BK21 (Brain Korea 21) project initiated by the Ministry of Education, and Unmanned Technology Research Center (UTRC) at Korea Advanced Institute of Science and Technology (KAIST), originally funded by DAPA, ADD.

REFERENCES

1. Choi J-W, Kim Y-H. Integral approach for reproduction of virtual sound source surrounded by loudspeaker array. IEEE trans. Audio, Speech, Lang. Process. 2012;20(7):1976-1989.
2. Choi J-W, Kim Y-H. Sound field reproduction of a virtual source inside a loudspeaker array with

minimal external radiation. IEEE trans. Audio, Speech, Lang. Process. 2013;21(2):247-259.
3. Boone MM, Verheijen E, Jansen G. Virtual reality by sound reproduction based on wave field synthesis. Proc 100th Conv. Audio Eng. Soc; 11-14 May 1996, Copenhagen, Denmark 1996. preprint 4145.
4. Verheijen E. Sound reproduction by wave field synthesis. Ph. D. dissertation, TU Delft, Delft, The Netherlands, 1998.
5. Song M-H. Prediction of localization error in generation of virtual source. Ph. D. dissertation, KAIST, Daejeon, Republic of Korea, 2013.
6. Berkhout AJ, de Vries D, Vogel P. Acoustic control by wave field synthesis. J Acoust Soc Am. 1993;93:2764-2778.
7. Ahrens J, Spors S. Focusing of virtual sound sources in Higher Order Ambisonics. Proc 124th Conv. Audio Eng. Soc; 17-20 May 2008, Amsterdam, The Netherlands 2008. preprint 7378.
8. Kang D-S, Lee J-M, Choi J-W, Song M-H, Kim Y-H. Virtual sound source generation: Its various methods and performances. Proc Int. Congresson Acoustics 2013; 2-7 June 2013; Montreal, Canada 2013.
9. Wittek H, Kerber S, Rumsey F, Theile G. Spatial perception in Wave Field Synthesis rendered sound fields: Distance of real and virtual nearby sources. Proc 116th Conv. Audio Eng. Soc; 8-11 May 2004, Berlin, Germany 2004. preprint 6000.
10. Volk F, Muhlbauer U, Fastl H. Minimum Audible Distance (MAD) by the example of Wave Field Synthesis, Proc DAGA2012; 19-22 March 2012, Darmstadt, Germany 2012. p. 319-20.
11. Coleman PD. An analysis of cues to auditory depth perception in free space. Psychological Bulletin. 1963;60(3):302-315.
12. Kopco N, Shinn-Cunningham BG. Effect of stimulus spectrum on distance perception for nearby sources. J Acoust Soc Am. 2011;130(3):1530-1541.
13. Nielsen S. Distance perception in hearing. Ph. D. dissertation, Aalborg University, Aalborg, Denmark, 1991.
14. Merson DH, King LE. Intensity and reverberation as factors in the auditory perception of egocentric distance," Percept. Psychophys. 1975;18:409-415.
15. Blauert J. Spatial Hearing. Massachusetts, London, England: MIT Press; 1997.
16. Hartley R, Fry T. The binaural location of pure tones. Physical Review. 1921;18:431-442.
17. Brungart DS, Rabinowitz WM. Auditory localization of nearby sources. II. Localization of a broadband source. J Acoust Soc Am. 1999;106(4):1956-1968.
18. Brungart DS, Rabinowitz WM. Auditory localization of nearby sources. III. Stimulus effects. J Acoust Soc Am. 1999;106(6):3589-3602.
19. Shinn-Cunningham BG, Kopco N, Martin TJ. Localizing nearby sound sources in a classroom: Binaural room impulse responses. J Acoust Soc Am. 2005;117(5):3100-3115.
20. Kim Y-H, Choi J-W. Sound visualization and manipulation. Singapore: Wiley & Sons; 2013. p. 320-332.
21. Duda RO, Martens WL. Range dependence of the response of a spherical head model. J Acoust Soc Am. 1998;104(5): 3048-3058.
22. Brungart DS, Rabinowitz WM. Auditory localization of nearby sources. Head-related transfer functions. J Acoust Soc Am. 1999;106(3): 1465-1479.
23. Shinn-Cunningham BG, Santarelli S, Kopco N. Tori of confusion: Binaural localization cues for sources within reach of a listener.
24. Williams EG. Fourier Acoustics. Cambridge, UK: Academic Press; 1999. p. 137-140.
25. Ward DB, Abhayapala TD. Reproduction of a plane-wave sound field using an array of loudspeakers, IEEE trans. Speech, Audio Process. 2001;9(6):697-707.